

Temperature dependence of macroscopic and microscopic PZT properties studied by thermo-mechanical analysis, dielectric measurements and X-ray diffraction

L. Seveyrat^{*}, M. Lemerrier, B. Guiffard, L. Lebrun, D. Guyomar

LGEF, INSA-Lyon, Bat G. Ferrié, 8 rue de la Physique, F-69621 Villeurbanne cedex, France

Received 17 April 2007; received in revised form 28 August 2007; accepted 6 September 2007

Available online 25 September 2007

Abstract

The main objective of the paper is to point out the influence of composition and of poling state (poled and unpoled samples) on the evolution of various parameters (ϵ_r , dilatation coefficients, lattice parameters) at different scales (lattice, bulk) using X-ray diffraction (XRD), thermo-mechanical analysis (TMA) and dielectric methods. The transition temperatures have been determined from the above measurements and compared. The composition has an influence on the transition temperature and not on the dilatation coefficient value. The poling state influences only the macroscopic dilatation evolution and not the value of the transition temperature. A scale effect is only observed on majoritary tetragonal compositions which show different values of transition temperatures from microscopic and macroscopic methods.

© 2007 Elsevier Ltd and Techna Group S.r.l. All rights reserved.

Keywords: B. X-ray methods; C. Dielectric properties; C. Thermal properties; D. PZT

1. Introduction

Ferroelectric lead zirconate titanate ceramics $\text{Pb}(\text{Zr}_x\text{Ti}_{1-x})\text{O}_3$ (abbreviated PZT) are largely used in sensing and actuating applications due to their remarkable piezoelectric and dielectric properties [1]. They have been the subject of extensive research in both experimental and theoretical physics. Above the Curie temperature (T_c), at which a reversible ferroelectric (polar) to paraelectric (non polar) phase transition occurs, perovskite-type PZT is cubic while below T_c it becomes tetragonal (T) for Ti-rich compositions or rhombohedral (R) for Zr-rich compositions. Generally, the composition range $x = 0.50$ – 0.54 , corresponds with the morphotropic phase boundary (MPB) separating the tetragonal from rhombohedral region. It is generally admitted that both T and R phases coexist in the MPB [2]. However, Noheda et al. [3] recently reported a new monoclinic phase in PZT materials by using X-ray synchrotron and Rietveld analysis. So the MPB is actually considered to be a mixture of T, R and monoclinic phases. Optimal dielectric and piezoelectric properties are obtained for

compositions in the vicinity of the MPB region [4], but the PZT performances may strongly be influenced by various external excitations: electric field, stress, temperature, etc. The paper deals with temperature dependence of some coefficients obtained from both microscopic and macroscopic measurements.

Four compositions of PZT ceramics with different Zr/Ti ratios were synthesized via a chemical route and characterized: 50/50, 52/48, 55/45 and 65/35. The first three Zr/Ti ratios correspond with MPB compositions, whereas the latter is purely rhombohedral.

The materials coefficients whose temperature dependence have been experimentally determined are:

- (1) Macroscopic ones: the dielectric constant, the linear dilatation and thermal dilatation coefficients.
- (2) Microscopic (structural) ones: the lattice parameters.

The evolution of the properties was discussed and the ferroelectric to paraelectric phase transition temperatures were estimated from the three methods for the four studied compositions. It is found that XRD measurements overestimate the phase transition temperature of majoritary

^{*} Corresponding author. Tel.: +33 4 72 43 89 92; fax: +33 4 72 43 88 74.

E-mail address: laurence.seveyrat@insa-lyon.fr (L. Seveyrat).

tetragonal compositions compared to those obtained by dielectric and dilatometric measurements.

2. Experimental procedure

PZT powders were prepared using an oxalate coprecipitation route [5], leading to stoichiometric and homogeneous materials. Tetra-*n*-butyl titanate, tetra-*n*-butyl zirconate were dissolved in a solution of oxalic acid. Lead acetate was added to this mix. After stirring, hydroxides and oxalates were precipitated with addition of ammonia. The product was calcinated at 600 °C for 10 h and then at 800 °C for 4 h.

After addition of 10% mass polyvinyl alcohol as a binder the powder was pressed into pellets of different sizes (disks and cylinders). The samples were heated at 600 °C for 4 h in order to eliminate the organic products and then sintered at 1250 °C for 6 h with a 2 °C/min heating rate. Ceramics were silver paste electroded on both opposite sides. When necessary, poling was made in a silicone oil bath at 150 °C for 1 min under an electric field applied along the axial direction. The field value was 3.5 kV/mm and 2.5 kV/mm for disks and cylindrical samples, respectively.

Dielectric constant (ϵ_r) was followed with an impedance-meter (HP 4284A) at 1 kHz, from room temperature to 500 °C with a heating rate of 1 °C/min.

X-ray diffraction data were obtained with a X'Pert Pro MPD Panalytical diffractometer using Cu K α radiation ($\lambda = 1.5406$ Å) with an incident-beam monochromator and a real time multiple strip X'Celerator detector. The diffraction patterns were recorded over the angular range 20–80° (2θ) with a step length of 0.016° (2θ) and a counting time of 100 s step⁻¹. The determination of cell parameters was carried out with X'Pert Plus software package supplied by Panalytical. X-ray studies were performed on disk samples (13 mm diameter, 0.5 mm thickness), silver paste electroded and poled when necessary. In this case, the electrodes were removed with solvent before X-ray diffraction measurement. For non-ambient studies, the diffractometer was equipped with an Anton Paar HTK16 high-temperature chamber, in which the thin disk was put directly in intimate thermal contact with a heating metal strip. So, as the ceramic is heated by thermal diffusion, it was necessary to use a previously temperature calibration, according to the following formula [6]:

true sample temperature (°C)

$$= \frac{\text{measured temperature (°C)} - 2.4761}{1.0568}$$

The X-ray diffraction was made on the disk surface perpendicular to the poling direction. Twenty-two isothermal scans were operated under ambient atmosphere (air) between room temperature and 600 °C. Before each scan the temperature is stabilized for 15 min.

The room temperature measurements were used to measure the phase ratio versus composition. The four studied PZT compositions differ from their Zr/Ti ratio: PZT 50/50, PZT 52/48, PZT 55/45 and PZT 65/35. Estimation of the volume fraction

of rhombohedral phase (F_R) was made from XRD reflections peaks deconvolution near $2\theta = 45^\circ$ by using the well known formula: $F_R = I_{(2\ 0\ 0)T}/I_{(2\ 0\ 0)R} + I_{(0\ 0\ 2)T}$, where $I_{(h\ k\ l)}$ is the intensity of the (*h k l*) peaks of the rhombohedral phase (*R*) and the tetragonal phase (*T*). Both PZT 50/50 and 52/48 exhibit majoritary tetragonal phase with F_R coefficient equal to 10 and 12%, respectively. As the PZT 55/45 shows a strong overlapping of the three reflection peaks, peak deconvolution was performed with a pseudo-Voigt profile function to estimate the peak intensities. The corresponding F_R coefficient was found to be about 50%. The PZT 65/35 is on the rhombohedral phase.

The length variations were studied with a thermo-mechanical analysis device (TMA96, Setaram) under air flow. The samples were cylindrical (6.35 mm diameter, 15 mm length). The linear dilation was measured along the cylinder axis which corresponds to the poling direction for poled samples. The measurement system consists in an alumina vertical spherical end compression type probe (force = 50 mN) associated with an electromagnetic transducer allowing a precision of 0.01 μm. As temperature sensor, a thermocouple (Pt:PtRh10%), located nearby the sample, at the same distance from each side was used.

For each composition, samples are submitted to a well defined temperature profile made of several on end phases:

- Phase one: Constant heating rate (1 °C/min) from room temperature to $T_i = 40$ °C and temperature stabilization at T_i for 2 h.
- Phase two: Constant heating rate (1 °C/min) from T_i to $T_{up} = 600$ °C and constant cooling rate (1 °C/min) from T_{up} to T_i .

As the measured length variation depends on sample, probe and apparatus frame behaviours, a reference experiment was performed using the same temperature profile and a reference alumina cylinder whose length equals the sample one.

3. Results and discussion

3.1. Macroscopic dielectric and dilatometric measurements

The Curie point T_c determined from the maximum of dielectric constant and the Curie temperature T_o obtained by extrapolation from the inverse dielectric constant are presented in Table 1. The values are compared with ones estimated from the following equation reported by Amin et al. [7] and Haun et al. [8] where x is the mole fraction of PbTiO₃: $T = (211.8 + 486.0x - 280.0x^2 + 74.42x^3)$ °C.

Table 1

Curie points T_c and Curie temperatures T_o obtained from dielectric measurements and compared with Amin results [7]

Zr/Ti	T_c (°C)	T_o (°C)	T [7] (°C)
50/50	398	398	394
52/48	393	394	389
55/45	387	386	381
65/35	359	360	351

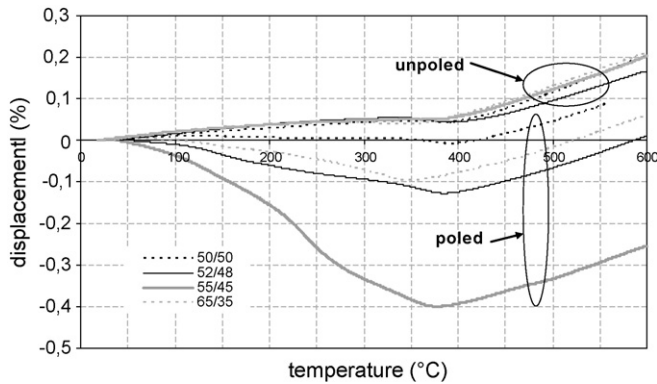


Fig. 1. Macroscopic dilatation vs. temperature for the four unpoled and poled samples.

It appears that the values of T_c and T_o temperatures are the same. It is coherent with second order phase transition [9], [10] which properties such as lattice constant, polarization or dielectric constant change continuously with temperature.

The transition temperatures measured on poled and unpoled ceramics have the same values. A well-known result is observed: the transition temperatures depend strongly on the ferroelectric material composition and the values increase with Ti content.

TMA supplies with the sample length variation ΔL and linear dilatation in the direction of symmetry axis (i.e. cylinder axis or (and) mean polarization direction). In order to get the polarization effect, unpoled and poled samples have been studied for each composition.

Fig. 1 shows the macroscopic linear dilatation for the four unpoled and poled ceramics.

All unpoled PZT compositions show a similar evolution of $\Delta L/l$ versus temperature. They present a slight expansion for $T < T_c$ and a stronger one for $T > T_c$. The low expansion in the ferroelectric phase region results from competition between PbZrO_3 expansion and contraction of PbTiO_3 . The negative thermal expansion of lead titanate is attributed to the decrease of anion-anion repulsion as polyhedra become more regular. One other explanation relies on the Ti–O bonds which are alternately long and short extending in linear chains along the c -axis and become equal in cubic form. As the unequal Ti–O bond lengths become equal, their average value decreases [11,12].

For unpoled samples the macroscopic polarization is equal to zero, due to the structure of the ceramic material (grains, domains, lattice) and the randomly spontaneous polarization directions of the microscopic domains. Nearby T_c the microscopic spontaneous polarisations or the number of domains decrease [13] and as a consequence generate a cell parameter contraction. It may be an explanation of the macroscopic zero dilatation or slight contraction observed just before T_c . The transition phase spreads some tens of degrees due the progressive dipolar moment variation and the heterogeneous structure of the ceramics.

If unpoled ceramics are supposed to be isotropic, poled samples get an anisotropy due to the macroscopic polarization in the direction of the cylinder axis.

Whereas an expansion is observed for the unpoled samples, the poled samples show a contraction when heating from T_i to T_c , as it is shown in Fig. 1.

This contraction is due to the re-orientation of the domains which have been previously oriented during the poling step. The strongest deformation is observed for the compositions close to the MPB especially for the 55/45 composition. For this composition the evolution of d/l shows an inflexion point near 250 °C that can be related to the rhombohedral/tetragonal phase transition.

Above the ferroelectric to paraelectric phase transition all the poled samples expand. The same expansion is observed for unpoled and poled ceramics.

The linear dilatation coefficients [$\alpha = 1/l(\Delta l/\Delta T)$] have been calculated from filtered DL curve in order to have a more precise determination of transition temperature. Indeed α increases strongly as the transformation occurs. The mean temperature of the interval of α strong variation corresponds to the phase transition temperature.

With this method the ferroelectric to paraelectric transition temperatures are 389, 384, 373 and 348 °C for respectively 50/50, 52/48, 55/45 and 65/35 poled ceramics. The precision of measurement can be estimated as ± 5 °C.

The same determination has been made on unpoled samples and leads to quasi identical results but it's a little more difficult due to the more slightly change of d/l and α on this region.

From these macroscopic dilatation measurements we have shown that the poling state has a great influence on the macroscopic dilatation evolution but not on the value of the transition temperature.

3.2. Microscopic dilatation measurements

Fig. 2 shows the evolution of the tetragonal, pseudo-cubic and cubic cell parameters obtained after refinement versus temperature for the four PZT.

In the temperature range from room temperature to the Curie point, the a parameter slightly increases and the c parameter decreases more strongly for the two tetragonal PZTs. The c -axis thermal contraction is not large enough to give a volume contraction. So it is observed a very small volume expansion. After the Curie point, the cell is cubic and the a parameter linearly increases.

The evolution is very different for the 55/45 and 65/35 PZT. For more facility the cell parameters have been refined using pseudo-cubic cell for these two compositions. In the temperature range from room temperature to the Curie point the cell parameter strongly decreases. The rhombohedral phase shows a higher lattice deformation than the tetragonal one when the temperature increases.

There is only a slight difference between unpoled and poled samples cell parameters evolution.

From these results it appears that the transition phase temperature which is pointed out by a large change in the evolution of the cell parameters is comprised between 350 and 450 °C for the four compositions.

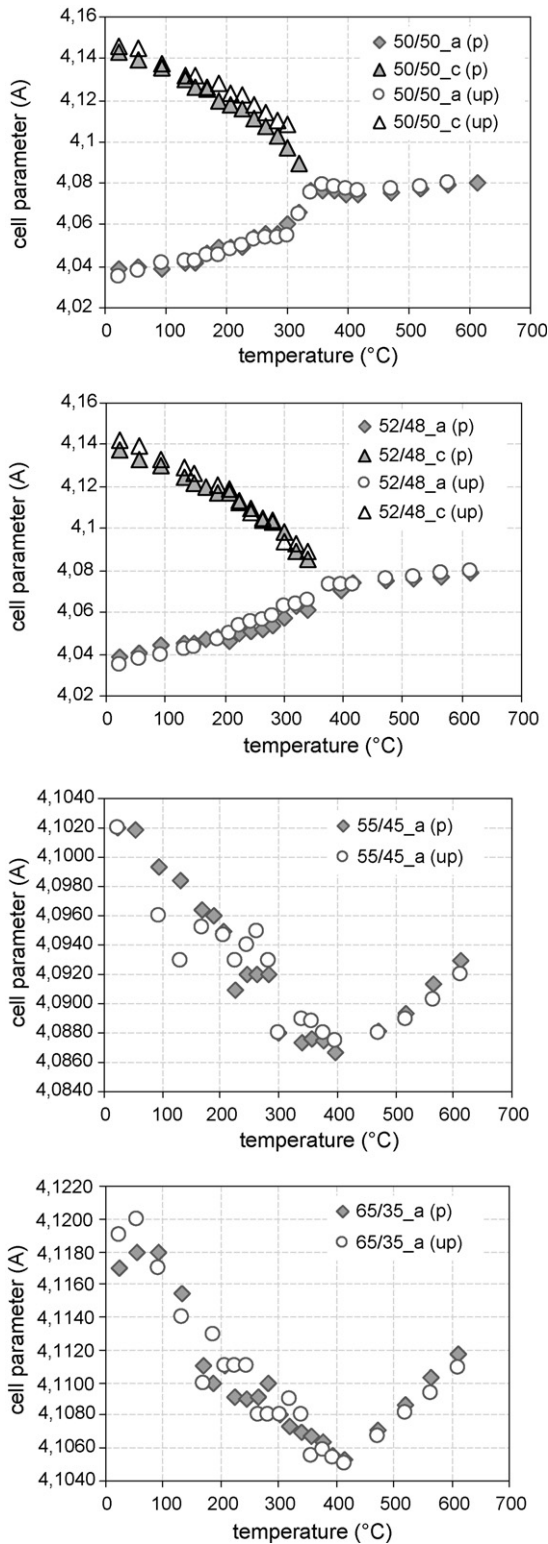


Fig. 2. Evolution of the a and c lattice parameters vs. temperature for unpoled (up) and poled (p) compositions.

For a more precise estimation of this temperature, the lattice plains reflections have been examined. They show very large changes when the temperature increases. For example Fig. 3 presents the XRD spectra from $2\theta = 36^\circ$ to $2\theta = 52^\circ$ for the 55/45 PZT.

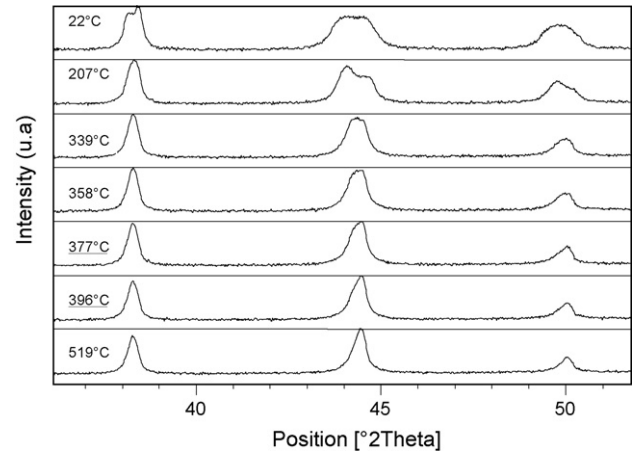


Fig. 3. XRD diagrams ($2\theta = 36\text{--}52^\circ$) for the 55/45 composition at different temperatures from room temperature to 520°C .

The room temperature X-ray diagram shows a mixture of tetragonal and rhombohedral phase. Near 200°C the symmetry is tetragonal. The transition phase from the tetragonal to cubic symmetry occurs between 377 and 396°C . After 396°C the cell is cubic: all the reflections have the same FWHM (full-width at half maximum). As discussed by Law et al. [14], the temperature at which the pseudo-cubic profile appears indicates the beginning of the destabilization of tetragonal phase. Above this temperature the samples cannot retain the domain alignment because of the dominant randomizing effect of the thermal energy.

From the same analysis of FWHM, the transition phase temperatures were estimated to be $457 \pm 28^\circ\text{C}$, $415 \pm 19^\circ\text{C}$, $387 \pm 19^\circ\text{C}$ and $358^\circ\text{C} \pm 19^\circ\text{C}$, respectively for 50/50, 52/48, 55/45 and 65/35 PZT. No difference is observed between unpoled and poled samples.

3.3. Comparison of transition temperatures obtained from microscopic and macroscopic methods

The ferroelectric to paraelectric phase transition temperatures determined from XRD, dielectric and TMA measurements

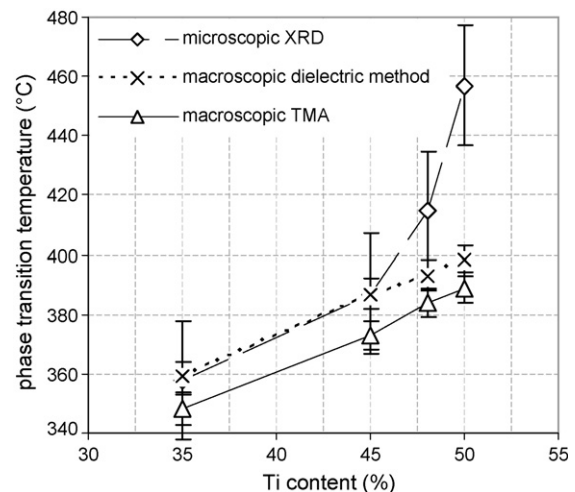


Fig. 4. Evolution of the phase transition temperatures obtained from both microscopic and macroscopic methods vs. the Ti content.

versus the Ti content are compared in Fig. 4. No or only a very slight difference is observed in the temperature determined on both poled and unpoled samples.

The two macroscopic methods lead to a linear evolution and very similar phase transition temperatures. The microscopic XRD method shows a more pronounced difference especially for the tetragonal compositions. For these compositions the phase transition temperature values are higher than macroscopic values. It is in accordance with the results of Franke et al. [15] who finds a pure cubic symmetry from X-ray diffraction studies at least 70 °C above the Curie temperature. It could be linked to the existence of micro-polar regions or clusters which are probably due to short-range order in the Pb sub-lattice which has a local structure different from that arising in long-range interactions.

4. Conclusions

The work has shown that the evolution in temperature of characteristic parameters can be influenced by the ferroelectric material composition and by the poling state. The composition has an influence on the transition temperature and not on the dilatation coefficient value. The poling state influences only the macroscopic dilatation evolution and not the value of the transition temperature. A scale effect is only observed on majoritary tetragonal compositions which show different values of transition temperatures from microscopic and macroscopic methods.

References

- [1] B. Jaffe, W.R. Cook, H. Jaffe, *Piezoelectric Ceramics*, Academic Press, New York, 1971.
- [2] S.K. Mishra, A.P. Singh, D. Pandey, 1997 Thermodynamic nature of phase transitions in $\text{Pb}(\text{Zr}_x\text{Ti}_{1-x})\text{O}_3$ ceramics near the morphotropic phase boundary I. Structural studies, *Philosoph. Magazine B* 76 (2) (1997) 213–226.
- [3] D.E. Noheda, G. Cox, G. Shirane, J.A. Gonzalo, L.E. Cross, S.E. Park, A monoclinic ferroelectric phase in the $\text{Pb}(\text{Zr}_{1-x}\text{Ti}_x)\text{O}_3$ solid solutions, *Appl. Phys. Lett.* 74 (1999) 2059–2061.
- [4] R. Guo, L.E. Cross, S.E. Park, B. Noheda, D.E. Cox, G. Shirane, Origin of the high piezoelectric response in $\text{Pb}(\text{Zr}_{1-x}\text{Ti}_x)\text{O}_3$, *Phys. Rev. Lett.* 84 (2000) 5423–5426.
- [5] B. Guiffard, M. Troccaz, Low temperature synthesis of stoichiometric and homogeneous lead zirconate titanate powder by oxalate and hydroxide coprecipitation, *Mater. Res. Bull.* 33 (12) (1998) 1759–1768.
- [6] L. Simon-Seveyrat, A. Hajjajji, Y. Emziane, B. Guiffard, D. Guyomar, Re-investigation of synthesis of BaTiO_3 by conventional solid state reaction and oxalate coprecipitation route for piezoelectric applications, *Cer. Int.* 33 (2007) 35–40.
- [7] A. Amin, M.J. Haun, B. Badger, A. McKinstry, L.E. Cross, A phenomenological Gibbs function for the single cell region of the lead zirconate (PbZrO_3): lead titanate (PbTiO_3) solid solution system, *Ferroelectrics* 65 (1985) 107–130.
- [8] M.J. Haun, E. Furman, H.A. McKinstry, L.E. Cross, Thermodynamic theory of the lead zirconate-titanate solid solution system, Part II: tricritical behaviour, *Ferroelectrics* 99 (1989) 27–44.
- [9] X. Dai, Z. Xu, D. Viehland, Effect of oxygen octahedron rotations on the phase stability, transformational characteristics, and polarization behavior in the lead zirconate titanate crystalline solution series, *J. Am. Ceram. Soc.* 78 (10) (1995) 2815–2827.
- [10] V.V. Eremkin, V.G. Smotrakov, E.G. Fesenko, 1990 Structure phase transition in $\text{PbZr}_{1-x}\text{Ti}_x\text{O}_3$, *Ferroelectrics* 110 (1990) 137–144.
- [11] A.W. Sleight, Compounds that contract on heating, *Inorg. Chem.* 37 (1998) 2854–2860.
- [12] X. Xing, J. Deng, J. Chen, G. Liu, Novel thermal expansion of lead titanate, *Rare Metals* 22 (4) (2003) 1–4.
- [13] L. Eyraud, *BaTiO₃ Diélectriques solides anisotropes et ferroélectricité*, Gauthier-Villars, Paris, 1967, Chap. VI Ferroélectricité.
- [14] H.H. Law, P.L. Rossiter, P.L. Simon, J. Unsworth, A model for the structural hysteresis in poling and thermal depoling of PZT ceramics, *J. Mater. Sci.* 30 (12) (1995) 4901–4905.
- [15] I. Franke, K. Roleder, J. Klimontko, A. Ratuszna, A. Soszynski, Anomalous piezoelectric and elastic properties of a tetragonal PZT ceramic near morphotropic phase boundary, *J. Phys. D: Appl. Phys.* 38 (2005) 749–753.